Virology 417 (2011) 369–378

Contents lists available at ScienceDirect

Virology

journal homepage: www.elsevier.com/locate/yviro

The interaction of flavivirus M protein with light chain Tctex-1 of human dynein plays a role in late stages of virus replication

Jean-Baptiste Brault [a], Mateusz Kudelko [b], Pierre-Olivier Vidalain [c], Frédéric Tangy [c], Philippe Desprès [a], Nathalie Pardigon [a,*]

[a] Unité des Interactions Moléculaires Flavivirus-Hôtes, Department of Virology, Institut Pasteur, 75724 Paris, France
[b] HKU-Pasteur Research Centre, The University of Hong Kong, Hong Kong, China
[c] Unité de Génomique Virale et Vaccination, Department of Virology, Institut Pasteur, CNRS URA 3015, 75724 Paris, France

ARTICLE INFO

Article history:
Received 22 March 2011
Accepted 22 June 2011
Available online 20 July 2011

Keywords:
Flavivirus
Membrane protein
Dynein light chain
Recombinant subviral particles (RSPs)
Virus trafficking

ABSTRACT

The role of the membrane protein (prM/M) in flavivirus life cycle remains unclear. Here, we identified a cellular interactor to the 40-residue-long ectodomain of prM/M (ectoM) using a yeast two-hybrid screen against a human cDNA library and GST pull-down assays. We showed that dynein light chain Tctex-1 interacts with the ectoM of dengue 1–4, West Nile, and Japanese encephalitis flaviviruses. No interaction was found with yellow fever and tick-borne flaviviruses. This interaction is highly specific since a single amino-acid change in the ectoM abrogates the interaction with Tctex-1. To understand the role of this interaction, silencing of Tctex-1 using siRNA was performed prior to infection. A significant decrease in progeny production was observed for dengue and West Nile viruses. Silencing Tctex-1 inhibited the production of recombinant dengue subviral particles (RSPs). Thus Tctex-1 may play a role in late stages of viral replication through its interaction with the membrane protein.

Introduction

Flaviviruses such as dengue (DENV), West Nile (WNV), Japanese encephalitis (JEV) and yellow fever (YFV) viruses are arthropod-borne pathogens (arboviruses) that are transmitted through the bite of an infected mosquito and may cause serious human diseases worldwide (Lindenbach et al., 2007). Outbreaks range from non-specific febrile illness to severe hemorrhagic (DENV and YFV) or encephalitic (JEV and WNV) syndromes. Arboviruses are becoming important public and veterinary health problems in several parts of the world, with numerous fatal cases reported. There is no available vaccine or efficient treatment against DENV and WNV.

Flaviviruses belong to the *Flaviviridae* family and are small enveloped viruses that have a genome composed of a single-stranded positive sense RNA of approximately 11 kb. The genome encodes a polyprotein that is cleaved by host and viral proteases to generate viral mature proteins, including 3 structural proteins (capsid (C), membrane (M) and envelope (E) and 7 non-structural proteins (NS1, NS2A, NS2B, NS3, NS4A, NS4B and NS5)) (Lindenbach et al., 2007).

The membrane protein is synthesized as a precursor prM. The cleavage of prM into the pr domain and M takes place in the trans-golgian compartment (Chambers et al., 1990; Stadler et al., 1997; Wengler, 1989; Westaway and Goodman, 1987), just prior to the production of mature virions, and this step is mandatory to generate infectious particles (Chambers et al., 1990; Elshuber et al., 2003; Lindenbach et al., 2007). The mature M protein thereby generated consists of a 40 amino-acid long ectodomain (coined ectoM) followed by 2 transmembrane domains (TMDs) (Chambers et al., 1990).

Our understanding of the functions played by the membrane protein remains quite evasive. Indeed, only a few studies described a biological role for it. To date, it has been shown that prM protein acts as a chaperone for the E protein folding (Konishi and Mason, 1993; Lorenz et al., 2002) and that the pr domain remains associated to the fusion loop of the E protein after cleavage of prM to prevent fusion within the infected cell (Yu et al., 2009). We and others have shown that ectoM of DENV M protein is a potent inducer of apoptosis through a mitochondrial-dependent pathway (Brabant et al., 2009; Catteau et al., 2003a, 2003b). Very recently, it was shown that the C-terminal helical domain of ectoM is involved in virus assembly and entry (Hsieh et al., 2011).

In this study, we sought to find cellular factors able to interact with the membrane protein in order to better understand its role during flaviviral life cycle. By using the ectoM of several flaviviruses as baits in a series of yeast-two hybrid (Y2H) screens performed against a human cDNA library, we identified Tctex-1, a dynein light chain (DLC), as an interactor of the ectoM of DENV, WNV and JEV. This cellular protein was previously involved in viral transport during herpes simplex virus (Douglas et al., 2004) and poliovirus (Mueller

* Corresponding author at: Unité Interactions Moléculaires Flavivirus-Hôtes, Department of Virology, Institut Pasteur, 25 rue du Docteur Roux, 75724 Paris, CEDEX 15, France. Fax: +33 1 40 61 37 74.
E-mail address: nathalie.pardigon@pasteur.fr (N. Pardigon).

0042-6822/$ – see front matter © 2011 Elsevier Inc. All rights reserved.
doi:10.1016/j.virol.2011.06.022

et al., 2002) infections. Using RNA interference against Tctex-1, we demonstrate that the ectoM interaction with Tctex-1 plays a role in the flaviviral life cycle, most likely during the trafficking of flaviviral particles within infected cells.

Results

Tctex-1 is a novel cellular protein interactor of DENV, JEV and WNV ectoM

In order to identify novel host factor(s) able to interact with the flavivirus membrane protein, we used the ectoM (the ectodomain of M protein without TMDs) from the four serotypes of DENV (DENV1–4), JEV, WNV, YFV and the live attenuated strain YFV17D as baits in a series of yeast two-hybrid (Y2H) screens against a human spleen cDNA library. Among host proteins captured with viral ectoMs as baits, only the DLC Tctex-type 1 (Tctex-1) was identified in the different screens by multiple virus species including DENV1, DENV2, DENV4, JEV, and WNV. This interaction was supported by only 1 to 10 yeast positive colonies in each individual ectoM screen (data not shown), suggesting that Tctex-1 frequency in the human cDNA library is relatively low. This could explain why Y2H screens performed with DENV-3, YFV, and YFV17D failed to identify this interaction. To address this issue and further validate these interactions, ectoM from all 8 viruses was systematically retested for Tctex-1 binding in the Y2H system (Fig. 1A). Yeast cells were co-transformed with each ectoM fused to the DNA binding domain of Gal4 (DB-ectoM) and Tctex-1 fused to the transactivation domain of

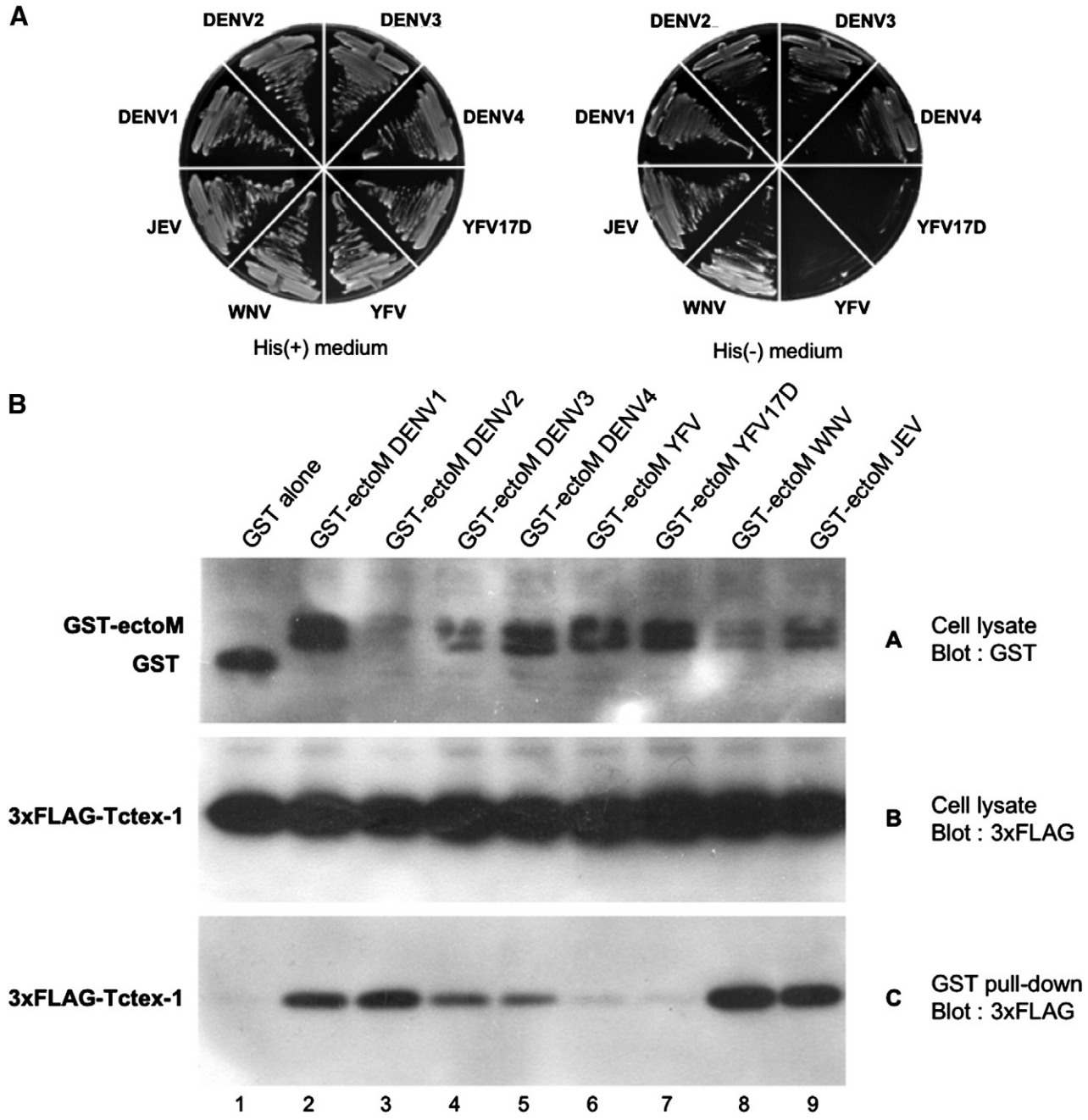

Fig. 1. Interaction of Tctex-1 with the ectoM of DENV1–4, WNV and JEV. (A) Y2H yeast strains expressing Gal4-DB fused to ectoM proteins from tested flavivirus were co-transformed to express Gal4-AD fused to Tctex-1. Cells were plated on synthetic medium lacking histidine so that yeast growth is determined by ectoM interaction with Tctex-1 and activation of *HIS3* reporter gene. (B) HEK-293T cells were co-transfected with 2 μg of a plasmid encoding the ectoM from tested flavivirus fused to GST or GST alone and 2 μg of a plasmid encoding Tctex-1 fused to 3xFLAG. 48 h post-transfection, cells were harvested and GST pull-down experiments were performed. Expression of both fusion proteins was detected by Western blot using antibodies directed against GST (panel A) and 3xFLAG (panel B). Presence of 3xFLAG-Tctex-1 after pull-down was then detected (panel C).

Gal4 (AD-Tctex-1). Yeast co-transformation was assessed on a synthetic medium depleted for leucine and tryptophan where yeast growth necessitates the presence of both bait and prey plasmids (Fig. 1A, His(+) medium). On a synthetic medium that is also missing histidine, and where yeast growth depends on ectoM interaction with Tctex-1, we confirmed Tctex-1 binding to ectoM from WNV and JEV (Fig. 1A, His(−) medium). In this pairwise setting, ectoMs from all DENV serotypes including DENV-3 were also found to interact with Tctex-1. This suggests that Tctex-1 interaction with DENV-3 was not identified in first instance because of technical limitations, which probably relate to the low frequency of Tctex-1 in the library. On the other hand, we confirmed that ectoM of YFV and YFV17D do not interact with this cellular protein, indicating that ectoM has distinct interaction properties among flaviviruses regarding Tctex-1. The same experiments were performed using the WNV pr domain alone or fused to ectoM. Interestingly, the pr-ectoM peptide also had the ability to interact with Tctex-1 while it was not the case for the pr domain alone, suggesting that ectoM is sufficient to promote the interaction with Tctex-1 but that it also occurs in the presence of the pr domain (data not shown). To confirm the interaction of Tctex-1 with ectoM, we performed pull-down experiments using plasmids encoding each of the ectoM sequences used in the Y2H screens fused to glutathione-S-transferase (GST) (Fig. 1B, panel A) and a plasmid encoding Tctex-1 fused to 3xFLAG (Fig. 1B, panel B). We observed that in agreement with the Y2H results DENV (1–4), WNV and JEV ectoM did interact with Tctex-1 (Fig. 1B, panel C, lanes 2, 3, 4, 5, 8 and 9 respectively). On the other hand, after pulling down the GST-fused ectoM of YFV and YFV17D, Tctex-1 signal was very weak compared to the other ectoM (Fig. 1, panel C, lanes 6 and 7), confirming our results obtained with the Y2H screens. Even though the level of expression of GST-ectoM is variable depending on the construct, it does not reflect on the ability of a given ectoM to interact or not with Tctex-1 as it can be seen for GST-ectoM-DENV2 compared to GST-ectoM YFV or YFV17D (Fig. 1, lane 3 compared to lanes 6 or 7). These results, obtained by using two distinct techniques, show that the ectoM of the four DENV serotypes, JEV and WNV are able to interact *in vitro* with the DLC Tctex-1 while the ectoM of YFV or YFV17D is not.

The amino acid residue in position 5 within the ectoM of WNV is essential for the interaction with Tctex-1

We then sought to identify the critical amino acids involved in the molecular interaction of flavivirus ectoM sequences with Tctex-1. Alignment of amino acid sequences indicated that WNV (interacting with Tctex-1) and YFV (not interacting with Tctex-1) ectoM displayed identical amino acids at positions 6, 7, 12, 19, 20, 27, 29, 31, 33, 35, 38–40 (Fig. 2A, blue boxes). We hypothesized that some residues in YFV ectoM that differed in WNV ectoM and in all the other ectoM sequences tested could interfere with the capacity of WNV ectoM to interact with Tctex-1. The proximal region of ectoM that encompassed amino acids 1 to 8 was targeted for mutation. Amino acid substitutions Ser to Ala at position 1, Thr to Asp at position 3, Gln to Pro at position 5, and Gly to Glu at position 8 altogether (Fig. 2A, red boxes) abrogated the interaction of WNV ectoM with Tctex-1 by GST pull-down assay (data not shown). This result suggested that the N-terminal region of WNV ectoM plays an important role in its ability to interact with Tctex-1. We then tested each amino-acid substitution separately, and found that a Gln to Pro mutation at position 5 (Fig. 2A, *) was the only substitution that abolished Tctex-1 interaction with WNV ectoM (Fig. 2B, panel C, compare lane 3 to lane 2). To further confirm the importance of this amino acid residue in the interaction with Tctex-1, we examined the capacity of ectoM from Kyasanur Forest disease virus (KFDV), Omsk hemorrhagic fever virus (OHFV), and tick-borne encephalitis virus (TBEV), all arboviruses carrying a Pro at position 5 in their ectoM sequence, to interact with Tctex-1 by GST pull-down assay and compared it with the ectoM of Usutu virus (USUV), a closely related virus to WNV carrying a Gln residue at this position (Fig. 2C). Remarkably, all ectoMs that contain a Pro residue at position 5 were unable to interact with Tctex-1, while the only ectoM not carrying it was able to do so (Fig. 2D, panel C, lanes 2, 4 and 5 compared to lane 3). These results support the hypothesis that amino acid at position 5 is a critical determinant of interaction of ectoM with Tctex-1. Most importantly, this demonstrated that Tctex-1 interaction with the ectoM from a subset of flavivirus is highly specific, and can be disrupted by a single amino acid change.

Local concentration of Tctex-1 is found close to sites of DENV assembly expressing prM protein

Subcellular localization of Tctex-1 and prM proteins was then assessed in DENV infected-cells. For this purpose, HEK-293A cells were infected with DENV for 24 h at a multiplicity of infection (MOI) of 1 particle per cell. The subcellular localization of prM protein was analyzed using 14E9 antibody, which is specific for DENV prM. Tctex-1 subcellular localization was analyzed using R5205 rabbit polyclonal antiserum. The pattern of both staining was observed by indirect immuno-fluorescence using a confocal microscope in a sequential acquisition mode (Fig. 3). Our results show that Tctex-1 concentrates in the vicinity of prM-expressing structures in DENV-infected cells, structures that might be sites of viral morphogenesis (see arrowheads, Fig. 3, upper panel). Magnification of infected cells (see framed cells in bottom panel) confirmed that the antibody directed against prM protein stains a perinuclear region where Tctex-1 seems to be largely expressed.

Tctex-1 is important for DENV and WNV progeny virus production

To determine whether Tctex-1 has a relevant role during infection, we examined DENV, WNV and YFV progeny virus production from human cells in which expression of Tctex-1 had been knocked-down prior to infection. HepG2 cells were treated with a specific siRNA directed against Tctex-1 mRNA (siRNA Tctex-1) or with a non-targeting control (siRNA NT), and were infected 24 h post-treatment, either with DENV or YFV at a MOI of 1 (Fig. 4, panels A and C). HEK-293A cells were treated in the same way and infected with WNV at a MOI of 1 (Fig. 4, panel B). Viral titers were measured by focus immuno-detection assay (FIA) for DENV and WNV and by plaque assay for YFV.

Whereas the difference in YFV titer was not significant between cells treated with NT or Tctex-1 siRNA (Fig. 4C), we observed a 65% decrease in DENV titer in cells where Tctex-1 expression had been knocked-down (Fig. 4A). WNV titer also showed a similar decrease of about 70% (Fig. 4B). To control that silencing of Tctex-1 does not alter early stages of infection, for example entry, cells were treated with siRNA prior to infection and cells were stained for the E protein in an immuno-fluorescence assay 24 h post-infection. No significant difference was observed in the proportion of infected cells when treated with NT or Tctex-1 siRNA (data not shown). Taken together, these results indicate that Tctex-1 is involved in DENV and WNV life cycle, probably in late stages of the infection, whereas it does not seem to participate in YFV life cycle. These results are consistent with the Y2H and GST pull-down assays, as Tctex-1 showed the ability to interact with DENV and WNV ectoM, while no interaction was observed with YFV ectoM.

Tctex-1 participates in the production of DENV recombinant subviral particles independently from microtubule cytoskeleton

Since dynein has already been involved in viral transport and is also known to play a role in ER-to-Golgi transport, we hypothesized that DENV or WNV hijack Tctex-1 to participate in the trafficking of viral particles along the secretory pathway. To test this hypothesis we used a stable Hela cell line expressing DENV1 prM and E proteins

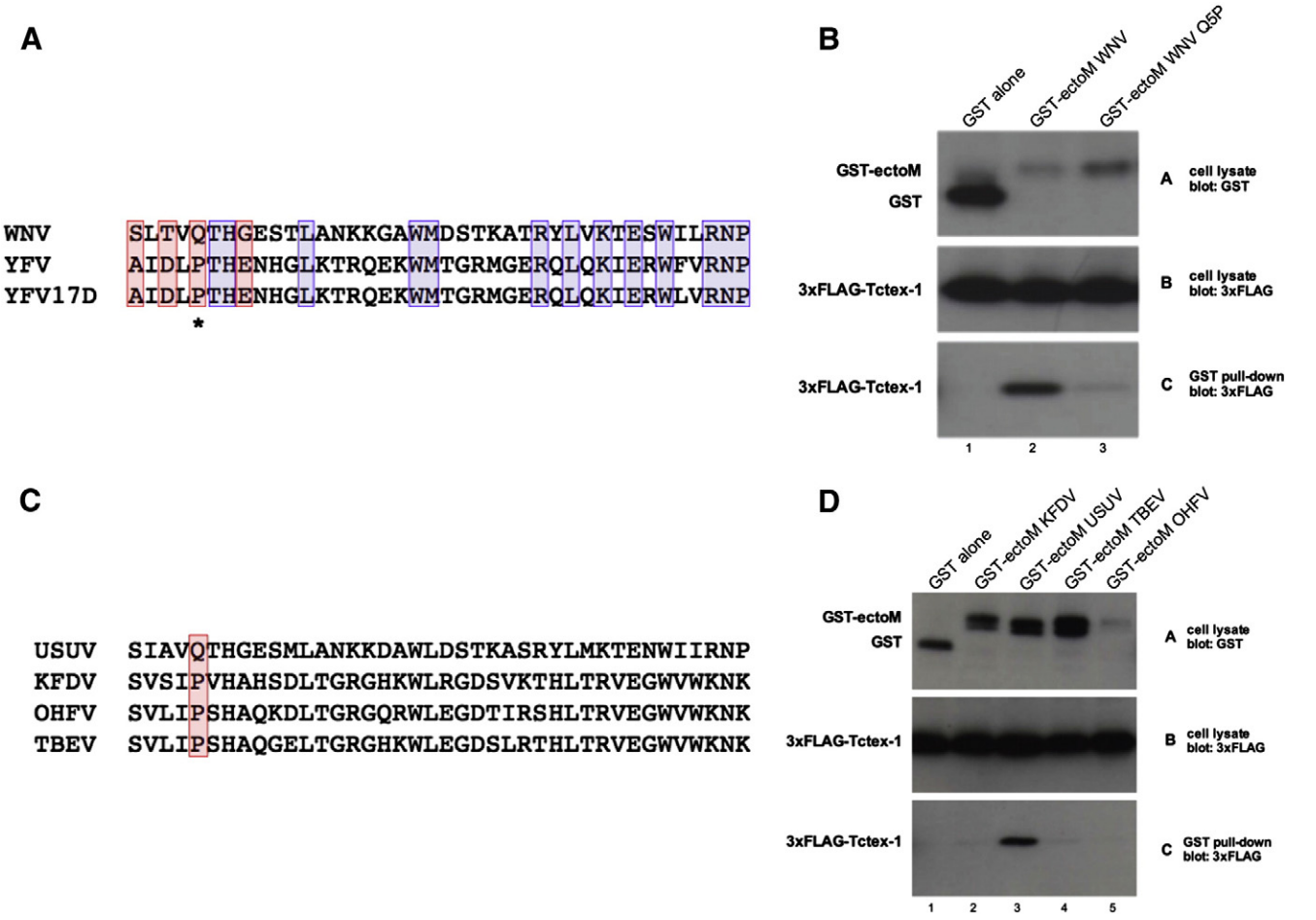

Fig. 2. The importance of amino acid 5 of WNV ectoM for the interaction with Tctex-1. (A) Alignment of WNV ectoM with YFV and YFV17D ectoM. Blue boxes represent identical amino-acids, red boxes represent different amino acids that were substituted within WNV ectoM with YFV residues. Asterisk pinpoints the only amino acid mutation that abrogates interaction of WNV ectoM with Tctex-1 (see B). (B) A mutant of WNV ectoM in which residue 5 was replaced with a proline (ectoM WNV Q5P) was generated by site-directed mutagenesis. HEK-293T cells were co-transfected with 2 μg of a plasmid encoding the ectoM of WNV, WNV Q5P fused to GST or GST alone and 2 μg of a plasmid encoding Tctex-1 fused to 3xFLAG. 48 h post-transfection, cells were harvested and GST pull-down experiments were performed. Expression of both fusion proteins was detected by Western blot using antibodies directed against GST (panel A) and 3xFLAG (panel B). The presence of 3xFLAG-Tctex-1 after pull-down was then detected (panel C). (C) The ectoM of 4 other flaviviruses containing a proline as residue 5 (Kyasanur Forest disease virus: KFDV, Tick-borne encephalitis virus: TBEV and Omsk hemorrhagic fever virus: OHFV) or not (Usutu virus: USUV) were also tested for their ability to interact with Tctex-1. Red box pinpoints residue 5. (D) HEK-293T cells were co-transfected with 2 μg of a plasmid encoding the ectoM of KFDV, USUV TBEV, OHFV fused to GST or GST alone and 2 μg of a plasmid encoding Tctex-1 fused to 3xFLAG. 48 h post-transfection, cells were harvested and GST pull-down experiments were performed. Expression of both fusion proteins was detected by Western blot using antibodies directed against GST (panel A) and 3xFLAG (panel B). The presence of 3xFLAG-Tctex-1 after pull-down was then detected (panel C).

(Hela prM-E) that was treated with NT or Tctex-1 siRNA. Hela prM-E cells assemble and secrete recombinant subviral particles (RSPs) undergoing maturation and trafficking processes similar to that of viral particles (Wang et al., 2009). To control Tctex-1 silencing efficiency, HEK-293T cells were co-transfected with a plasmid encoding Tctex-1 fused to 3xFLAG and NT or Tctex-1 siRNA. Tctex-1 expression was then observed by immunoblot assay using an antibody directed against the 3xFLAG tag (Fig. 5A). Compared to cells treated with NT siRNA (Fig. 5A, lane 1), cells treated with Tctex-1 siRNA (Fig. 5A, lane 2) show a significant reduction in 3xFLAG-Tctex-1 expression, confirming the efficiency of the siRNA. Hela prM-E cells were treated either with two increasing concentrations of NT or Tctex-1 siRNA. Cells were washed 24 h post-treatment to remove RSPs secreted during the treatment and incubated in fresh medium over-night. Supernatants were then collected and cells harvested. RSP expression and release were assessed by measuring E and prM protein expression in cell lysates and supernatants (Fig. 5B). Compared to cells transfected with NT siRNA, cells transfected with Tctex-1 siRNA show a reduction of E protein expression in supernatant (Fig. 5B, upper panel, lanes 3 and 4 compared to lanes 1 and 2), suggesting an inhibition of RSP secretion after Tctex-1 silencing. Compared to cells treated with NT siRNA, intracellular expression of E protein is also reduced after treatment with Tctex-1 siRNA (Fig. 5B, upper panel, lanes 7 and 8 compared to lanes 5 and 6). We can see the same effect on prM intracellular expression (Fig. 5B, lower panel, lanes 7 and 8 compared to lanes 5 and 6). The signal corresponding to prM disappears in supernatant, indicating an efficient cleavage of the protein before secretion of the particles (Fig. 5B, lower panel, lanes 1–4). These observations indicate that Tctex-1 is involved in DENV RSP production. To verify whether the Tctex-1 role in RSP production is related to its microtubule-dependent retrograde transport function within the dynein motor complex, we tested the impact of microtubule disruption on RSP production and release. Hela prM-E cells were treated with nocodazole (NZ), a drug that interferes with polymerization of microtubules. We observed a striking dismantling of the microtubule network in NZ-treated cells compared to mock-treated ones (Fig. 5C). RSP expression and release were then assessed after drug treatment by measuring the expression of the E protein in cell lysate and supernatant respectively (Fig. 5D). Despite microtubule destruction in NZ-treated cells, no difference was observed in E protein expression compared to mock-treated cells both in supernatant (Fig. 5D, lane 2 compared to lane 1) and cell lysate (Fig. 5D, lane 4

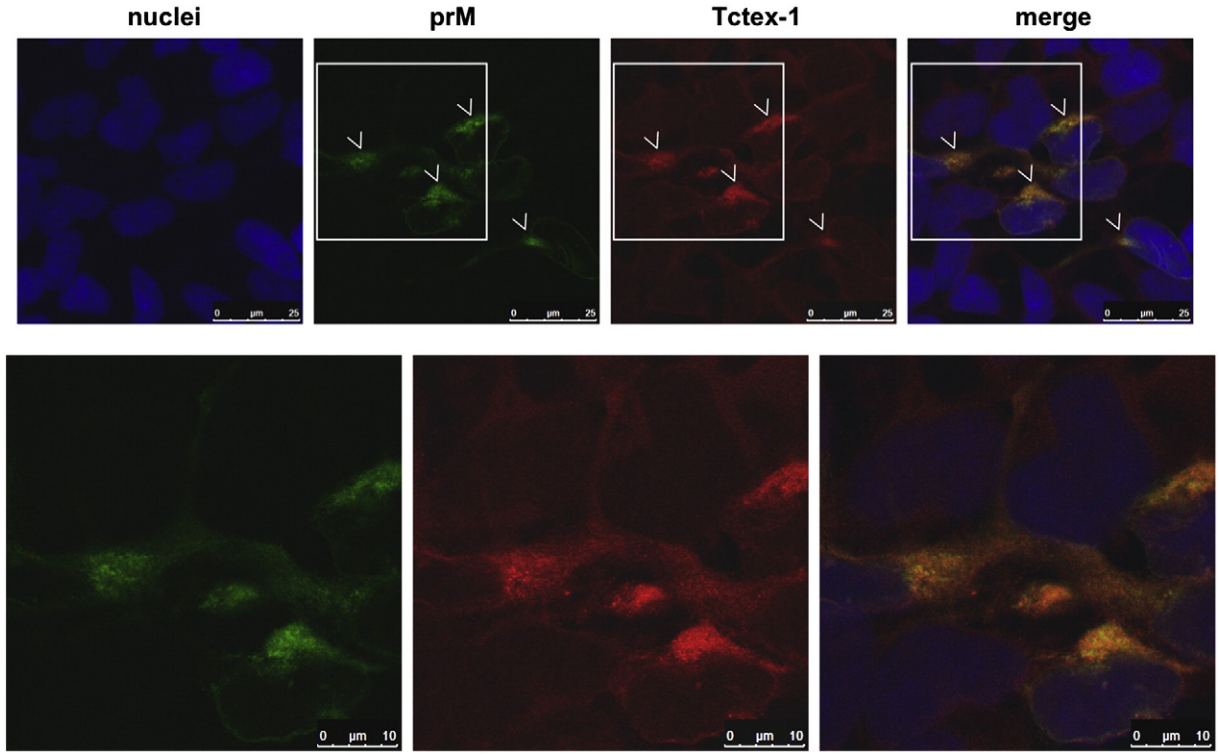

Fig. 3. Subcellular localization of Tctex-1 and prM proteins in DENV-infected cells. HEK-293A cells were infected at a MOI of 1 with DENV4 63632/76 Burma for 24 h. Cells were washed with PBS and fixed with 3.2% paraformaldehyde PBS. DENV prM and Tctex-1 protein were stained with 14E9 mAb and anti-Tctex-1 rabbit polyclonal antiserum R5205 respectively. Arrowheads point towards DENV-infected cells. Bottom panel represents magnification of framed cells in the upper panel. Pictures were taken using a Leica scanning confocal SP5 microscope in sequential acquisition mode.

compared to lane 3), indicating that microtubules are not involved in the production of RSPs. Altogether these results suggest that Tctex-1 plays a role in the production of DENV particles within the infected cells, in a way that is independent of microtubules and thus not related to microtubule-dependent retrograde transport of the dynein motor complex.

Discussion

Our study describes for the first time the identification of a host factor interacting with the membrane protein of several flaviviruses. We showed that Tctex-1 is important for DENV and WNV infection and is involved in the late steps of viral infection. We propose that these viruses have the ability to highjack Tctex-1 late in their life cycle via an interaction with the ectodomain of the M protein. The identification of novel host factors that flaviviruses hijack and use during infection is mandatory for a better comprehension of their pathogenicity. No vaccine or effective antiviral molecules are currently available to prevent or treat DENV or WNV infection, so there is an urgent need to better understand the pathogenesis of these viral infections. Protein–protein interactions define key biochemical and regulatory networks in the cell, but are also targets for a virus to ensure its life cycle as viruses are obligatory parasites. In this study, we identified Tctex-1 protein, a member of one of the 3 DLC families, as a partner for the ectodomain of DENV, WNV and JEV membrane protein. Our results suggest that the interaction between the ectoM and Tctex-1 is important for the DENV and WNV life cycle in human hepatic and kidney cells respectively and that Tctex-1 is involved in late stages of DENV infection. The involvement of DLC in viral transport had already been described. Indeed, Tctex-1 has been shown to participate in the targeting of Mason-Pfizer monkey virus polyprotein to its site of assembly (Vlach et al., 2008), to interact with Herpes simplex virus type 1 capsid protein VP26 and to participate in its cytoplasmic transport along microtubules (Douglas et al., 2004). It was also described to interact with the human Poliovirus (PV) receptor CD155 in order to ensure efficient retrograde transport of PV-containing vesicles along microtubules (Mueller et al., 2002; Ohka et al., 2004). Other DLC play a role in viral transport mechanisms. LC8 for example has been described as an interactor of rabies virus phosphoprotein P (Jacob et al., 2000; Raux et al., 2000) and African swine fever virus p54 protein (Alonso et al., 2001) and was described as being essential for foamy virus GAG protein (Petit et al., 2003) and bovine immunodeficiency virus retrograde transport mechanisms (Su et al., 2010).

The location where ectoM encounters Tctex-1 is unclear as the two proteins are expressed in different cellular compartments, Tctex-1 and ectoM being described as cytosolic and luminal, respectively. However, it was demonstrated recently that upon ER stress induction, ER membrane permeability occurs and endogenous ER luminal proteins may be released into the cytosol (Wang et al., 2011). Interestingly, the regulation of ER membrane permeability to luminal proteins is dependent of Bax protein, a pro-apoptotic factor that was described to be up-regulated during WNV and Saint-Louis encephalitis virus (SLEV) infection (Parquet et al., 2002, 2001). This mechanism may be involved in ER stress-induced apoptosis, possibly through translocation of factors from the ER lumen to the cell surface that could facilitate in yet unknown ways apoptotic signaling cascade. Knowing that flaviviruses like WNV, JEV or DENV activate the unfolded protein response (UPR), a cellular response induced by the stress due to accumulation of unfolded or misfolded proteins in the ER (Ambrose and Mackenzie, 2011; Yu et al., 2006) that can lead to ER stress-induced apoptosis (Medigeshi et al., 2007), it is possible that flaviviral proteins expressed in the ER may be in contact with the cytoplasm because of ER stress-induced membrane permeability, allowing them to meet with cytosolic proteins. Another hypothesis that could explain where the ectoM and Tctex-1 interact would be the

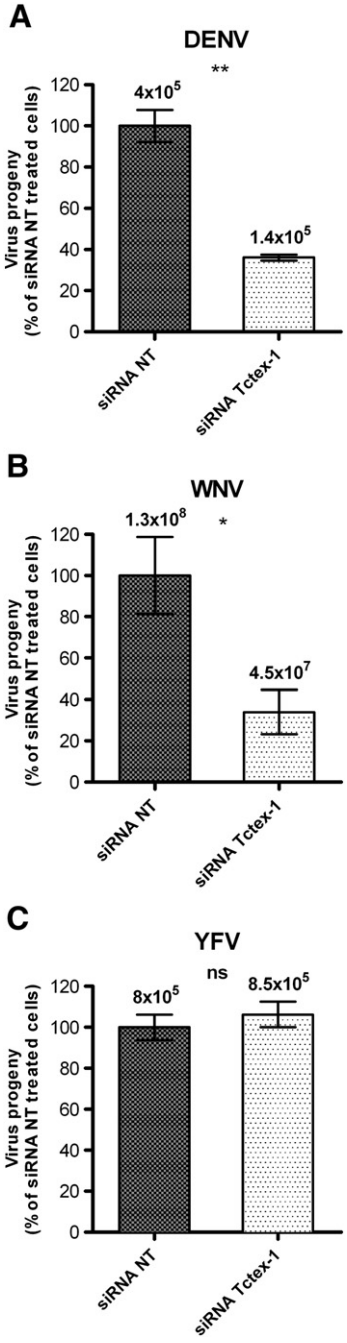

Fig. 4. Effect of Tctex-1 knockdown on virus progeny production. HepG2 or HEK-293A cells were transfected with 100 nM of NT or Tctex-1 siRNA. 24 h post-transfection, HepG2 cells were infected either with DENV or YFV at a MOI of 1 and HEK-293A cells were infected with WNV at the same MOI. 48 h post-infection, supernatants were collected, DENV (A) and WNV (B) progeny production was measured by Focus Immunodetection Assay, YFV (C) progeny production was measured by plaque assay. Difference between NT and Tctex-1 siRNA treated samples is only significant for DENV (**P = 0.0053) and WNV infected-cells (*P = 0.0491) according to *t*-test. For each virus, at least two distinct experiments were performed in triplicates. Values above each bar indicate the viral titer per milliliter of supernatant.

existence of a different membrane topology of prM protein. Some viral glycoproteins have already been described to adopt different transmembrane configurations. It is the case of hepatitis B virus (HBV) L envelope protein that exhibits a dual transmembrane topology with both luminal and cytosolic orientations (Prange and Streeck, 1995). This dual topology is regulated by a posttranslational translocation process of a L protein subdomain into the ER that involves chaperone proteins (Lambert and Prange, 2003). However, such a mechanism has yet never been described for flaviviruses.

As shown after treatment of cells expressing DENV RSPs with siRNA directed against Tctex-1, silencing leads to the decrease of both intracellular and extracellular expression of viral proteins. This result is surprising because if Tctex-1 is involved in viral trafficking steps, one would expect that upon Tctex-1 knockdown, viral components should accumulate within the cell and thus show an increase of intracellular expression level. However, one can argue that such an accumulation could lead to a stress of the ER resulting in degradation of accumulated viral proteins, explaining the decrease observed for the intracellular signal.

Tctex-1 involvement in viral particle trafficking may be linked to its ability to interact with Src family kinases (SFKs). Two different SFKs have been shown to be involved in flaviviruses maturation/trafficking mechanisms. In fact, c-Yes protein is required for maturation of WNV particles (Hirsch et al., 2005), and c-Src protein is important for assembly and secretion of DENV (Chu and Yang, 2007). Interestingly, Tctex-1 has been reported to interact with Fyn, a member of the SFK family (Campbell et al., 1998). Further experiments that are currently undertaken to determine whether Tctex-1 and SFK are working together during the infection may provide a greater comprehension of flavivirus infection maturation/trafficking steps. As it has already been described, microtubules seem not to be involved in the secretion of flaviviruses (Mackenzie and Westaway, 2001), since their complete disruption using nocodazole did not decrease RSP secretion. Such result suggests that the dynein motor complex is not engaged with Tctex-1 in the late stages of flavivirus replication. It was already shown that there is a subset of Tctex-1 protein that localizes to the Golgi apparatus and that is not associated with the dynein intermediate chain, indicating the existence of distinct Tctex-1 populations with different subcellular localizations (Tai et al., 1998). Other families of DLC have been reported to have dynein-independent functions. LC8 is known to sequester the proapoptotic factor Bim_L to the dynein motor complex. After an apoptotic stimulus, LC8 together with Bim_L are released from the motor complex and translocated to Bcl-2 to antagonize its anti-apoptotic activity (Puthalakath et al., 1999). These findings indicate that DLCs are able to exert different functions independently and away from their interaction with the dynein motor complex.

Finally, the fact that not all flavivirus ectoMs interact with Tctex-1 raises interrogations about viral chimeras used as potential vaccines. Chimeric viruses containing the backbone of the 17D vaccine strain of YFV and the prM-E region of DENV or WNV will thus exhibit the ectodomain of the M protein that interacts with Tctex-1, in the frame of a virus whose ectoM does not interact with Tctex-1 (namely YFV17D). This difference should be kept in mind and evaluated as such chimeric viruses are currently tested in immunization protocols.

In conclusion, our results formally identify DLC Tctex-1 as a cellular interactor to the M protein from DENV, JEV and WNV and suggest a major role for this interaction in the efficiency of virus replication in human cells. This finding enhances our understanding of flavivirus life cycle, since very few host proteins involved in late steps of flavivirus infection including assembly, trafficking and maturation have been identified.

Materials and methods

Cells, viruses, antibodies and reagents

HEK-293A, HEK-293T, HepG2 and Vero cells were cultured in DMEM medium (Invitrogen) supplemented with 10% heat-inactivated fetal calf serum (PAA) and 1% penicillin/streptomycin at 37 °C. Hela prM-E cell line expressing prM and E protein from DENV1 were cultured in the same medium supplemented with 500 μg/ml Hygromycin B as reported

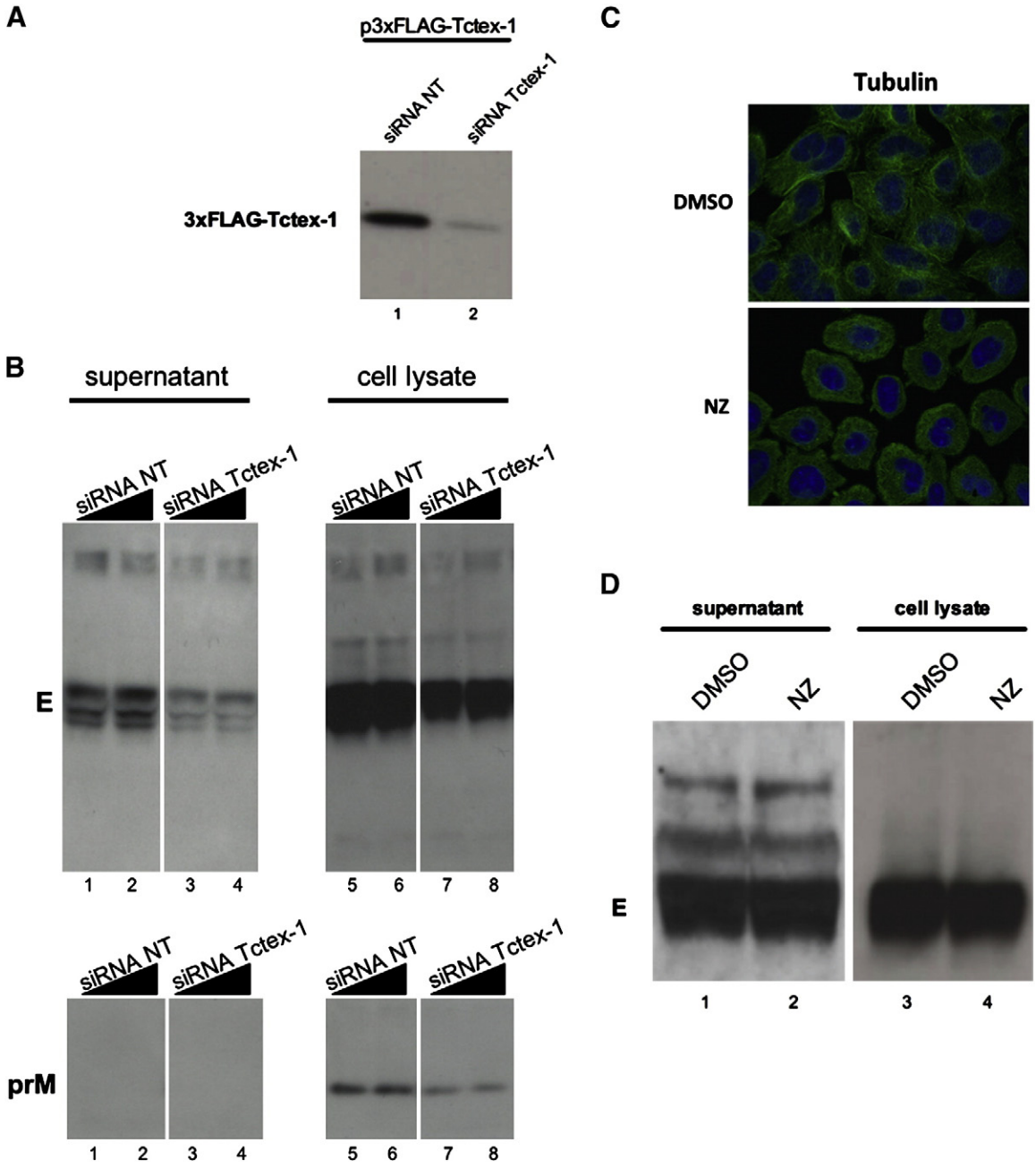

Fig. 5. The effect of Tctex-1 knockdown or microtubule disruption on DENV RSP production. (A) To control knockdown efficiency, HEK-293T cells were co-transfected with 2 μg of a plasmid encoding Tctex-1 fused to 3xFLAG and 100 nM of NT or Tctex-1 siRNA. 24 h post-transfection, Tctex-1 expression level was measured by Western blot using anti-3xFLAG antibody. (B) Hela prM-E cells expressing DENV1 recombinant subviral particles (RSP) were transfected with 100 nM and 200 nM of NT or Tctex-1 siRNA. Supernatants were collected and cell lysates harvested. The RSP level of expression was assessed in Western blot by measuring prM and E expression in cell lysate and supernatant using 14E9 and 4G2 antibodies respectively. (C) To control microtubule disruption efficiency Hela prM-E cells were treated with nocodazole (NZ) or with DMSO as a negative control for 1 h and then stained with DM1A antibody. (D) Hela prM-E cells were treated with NZ or DMSO as a negative control. RSP level of expression was measured by Western blot in cell lysate and supernatant using 4G2 antibody.

previously (Wang et al., 2009). Mosquito AP61 cells were cultured in Leibovitz's L-15 medium (Invitrogen) supplemented with 10% heat-inactivated fetal calf serum (PAA), 1% penicillin/streptomycin and 1% tryptose phosphate (Eurobio) at 28 °C.

The following virus strains from the collection of the Institut Pasteur were used to infect cells: DENV4 63632/76 Burma, WNV IS-98-ST1 and YFV Asibi.

Anti-3xFLAG HRP-conjugated, anti-αtubulin DM1A and DM1A-FITC conjugated monoclonal antibodies were purchased from Sigma-Aldrich. Anti-βtubulin goat antibodies were purchased from Abcam. Anti-GST HRP-conjugated goat antibodies were purchased from Amersham Biosciences. Anti-Tctex-1 rabbit polyclonal antiserum R5205 was kindly provided by Stephen M. King. 4G2 is a pan-flavivirus anti-E protein murine monoclonal antibody. 14E9 is a pan-dengue anti-prM protein murine monoclonal antibody. All the secondary antibodies were purchased from Jackson ImmunoResearch.

Nocodazole was purchased from Sigma Aldrich.

Yeast two-hybrid screen

Our yeast two-hybrid protocol has already been described in details (Caignard et al., 2007). Briefly, pDEST32 plasmid encoding Gal4-DB fused to ectoMs was transformed in AH109 yeast strain (Clontech), and used to screen by mating a human spleen cDNA

library cloned in the Gal4-AD pPC86 vector (Invitrogen) and previously established in Y187 yeast strain (Clontech). Yeast cells were plated on a selective medium lacking histidine to select for interaction-dependent transactivation of HIS3 reporter gene. AD-cDNAs from [His+] colonies were amplified by PCR and sequenced to identify the host proteins interacting with ectoM.

Construction of expression plasmids and transfection

All constructs were amplified using standard PCR methods (ExTaq, Takara) and cloned using a recombinational system (Gateway, Invitrogen) into pDONR207 (Invitrogen). PCR primers were used to amplify and clone viral or cellular ORF displayed from 20 to 30 specific nucleotides matching ORF extremities so that their Tm is close to 60 °C. To achieve recombinational cloning of PCR products, 5′ ends of forward primers were fused to attB1.1 recombination sequence 5′-GGGGACAACTTTGTACAAAAAAGTTGGCATG-3′, while reverse primers were fused to attB2.1 recombination sequence 5′-GGGGACAACTTTGTACAAGAAAGTTGGTTA-3′. Primer pairs were designed using the ViralOrfeome interface (http://www.viralorfeome.com; Pellet et al., 2010). Recombination of PCR products into pDONR207 was performed following manufacturer's recommendation (BP cloning reaction, Invitrogen). All constructs were transformed and amplified in *Escherichia coli* DH5α strain. Subsequently, viral ectoM and Tctex-1 sequences previously cloned into pDONR207 were transferred by recombinational reaction into Gateway compatible GST-fusion (pDEST27, Invitrogen) and 3xFLAG-fusion (pCI-neo-3xFLAG, Mendoza et al., 2006) destination vector respectively, following the manufacturer's recommendation (LR cloning reaction, Invitrogen). EctoM were amplified by PCR from viral preparations: DENV1 strain FGA/89 (Genbank ID: AF226687), DENV2 strain Jamaica/N.1409 (Genbank ID: M20558), DENV3 isolate D3/H/IMTSSA-SRI/2000/1266 (Genbank ID: AY099336), DENV4 strain Singapore 8976/95 (Genbank ID: AY762085), WNV strain NY99 flamingo 383–99 (Genbank ID: AF196835), JEV strain SA(V) (Genbank ID: D90194) and YFV strain 17D (Genbank ID: X03700). YFV Asibi ectoM was amplified from YFV strain 17D by site-directed mutagenesis allowing the transversion mutation of nucleotide 856 from C to A. EctoMs of USUV strain Vienna 2001 (Genbank ID: AY453411), KFDV variant Alkhurma (Genbank ID: NC_004355), OHFV (Genbank ID: NC_005062) and TBEV strain Neudoerfl (Genbank ID: U27495) as well as mutants of WNV ectoM were synthetic genes purchased from Genecust. Transfection was performed with Lipofectamine 2000 (Invitrogen) according to the manufacturer's recommendation.

GST pull-down

One day before transfection HEK-293T cells were seeded in 6 well plates at a density of 8.10^5 cells per well. Cells were transfected with 2 μg of p3xFLAG-Tctex-1 and 2 μg of pGST-ectoM or pGST per well. Cell layers were then harvested 48 h post-transfection using 300 μl of lysis buffer (0.5% NP-40, 20 mM Tris–HCl pH = 8, 120 mM NaCl and 1 mM EDTA) supplemented with Complete Protease Inhibitor Cocktail (Roche) per well. Lysates were incubated for 20 min at 4 °C and clarified by centrifugation. Lysates were then incubated with 20 μl of glutathione-sepharose beads (Amersham Biosciences) for 2 h at 4 °C and washed three times with 500 μl of ice-cold lysis buffer. Proteins were recovered by boiling in Nupage LDS sample buffer (Invitrogen) for 5 min at 95 °C.

Western blotting

Samples were separated on 4–12% Bis–Tris Gels (Invitrogen) and transferred on nitrocellulose membranes (Hybond-ECL, Amersham Biosciences). Membranes were blocked with 0.1% Tween 20, 5% milk PBS overnight at 4 °C and incubated with primary antibodies: anti-GST HRP conjugated (1:1000), anti-3xFLAG HRP conjugated (1:1000), anti-Tctex-1 rabbit polyclonal antiserum R5205 (1:100) or anti-αtubulin DM1A (1:1000) and when necessary with HRP conjugated donkey secondary antibodies (1:10 000) for 1 h at 4 °C in 0.1% Tween 20 PBS. Membranes were then revealed using ECL Plus Western Blotting Detection System and Hyperfilm ECL (Amersham Biosciences) according to manufacturer's recommended procedure.

Immunofluorescence

Cells were fixed in 3.2% paraformaldehyde (PFA) PBS for 15 min at room temperature. Cells were then washed three times in PBS and incubated in 50 mM NH_4Cl PBS for 15 min at room temperature to quench remaining PFA. Cells were washed three times in PBS and permeabilized in 0.1% Triton X-100 PBS for 5 min at room temperature. Cells were then washed three times in PBS and blocked with 2% bovine serum albumin (Sigma Aldrich) PBS for 30 min at room temperature. Cells were washed three times in PBS and incubated with anti-Tctex-1 rabbit polyclonal antiserum R5205 (1:50) and 14E9 mAb (1:200) in 0.1% Triton X-100 PBS for 1 h at room temperature. Cells were washed three times in PBS and were then incubated with goat anti-rabbit Alexa Fluor 546-conjugated (1:200) and donkey anti-mouse FITC-conjugated (1:200) secondary antibodies in 0.1% Triton X-100 PBS for 1 h at room temperature. Cells were washed three times in PBS and one time in a large volume of water to remove remaining salts. Samples were mounted in ProLong Gold antifade reagent with DAPI (Invitrogen).

Infection

One day before infection, cells were seeded in 24 well plates. Prior to infection cell layers were washed three times with DMEM without FCS. Virus solutions were prepared in DMEM supplemented with 2% of FCS at the required multiplicity of infection (MOI). 400 μl of the viral solution were used for each well and cells were incubated for 1 h 30 min at 37 °C. The inoculum was then discarded and replaced with 500 μl of 2% FCS DMEM and cells were incubated at 37 °C for 24 h or 48 h.

RNA interference

Non-targeting (NT) and anti-Tctex-1 mRNA (5′-CCAGUGGACCA-CAAAUGUATT-3′) siRNA duplexes were purchased from GeneCust. Reverse transfection protocol using Dharmafect 1 transfection medium (Dharmacon) was applied with 100 nM and 200 nM of siRNA. Mixtures of siRNA and transfection medium were made in DMEM and 200 μl were loaded in 24 well plates. 800 μl Hela prM-E (10^5 cells/ml), HepG2 or HEK-293A (2.10^5 cells/ml) in 2% FCS DMEM were added to each well and cells were incubated for 24 h at 37 °C.

Nocodazole treatment

One day before drug treatment Hela prM-E cells were seeded in 24 well plates at a density of 8.10^4 cells per well. Cell layers were washed once with 2% FCS DMEM and the same medium containing 2 μg/mL nocodazole was added. Cells were incubated for 1 h at 37 °C.

To control nocodazole efficiency, cells were fixed in ice-cold methanol and stained with DM1A FITC-conjugated (1:200) antibodies.

DENV RSP production and quantification

Hela prM-E cells were treated with siRNA or nocodazole. 24 h post siRNA transfection or 1 h post nocodazole treatment, Hela prM-E cells were washed three times with DMEM to remove all the RSP from the supernatant. 300 μl of 2% FCS DMEM was added to each well. SiRNA treated cells were incubated at 37 °C overnight. Nocodazole treated cells were incubated at 37 °C for 5 h. Supernatants were collected and

cell layers harvested with 100 µl of lysis buffer. Quantification of RSP in cell lysates and supernatants was performed by Western blot (see Western blotting section above).

Virus titration

DENV and WNV were titrated by focus immunodetection assay (FIA). One day before titration, AP61 cells were seeded in 24 well plates. One day after seeding, 10 fold serial dilutions of infectious supernatants in 10% FCS L-15 medium were made from 10^{-1} to 10^{-5} for DENV and to 10^{-6} for WNV. Cells were washed three times with L-15 medium without FCS and 200 µl of 2% FCS L-15 were added to each well. 200 µl of dilutions 10^{-2} to 10^{-5} for DENV and 10^{-3} to 10^{-6} for WNV were then added and cells were incubated for 2 h at 28 °C. In the meantime, a 1:1 solution of carboxy-methyl cellulose (CMC) and 10% FCS L-15 was prepared and 400 µl were added to each well. Cells infected with DENV were incubated for 5 days, cells infected with WNV for 3 days at 28 °C. Cells were then washed three times in PBS and fixed in 3% formaldehyde PBS for 20 min at room temperature. Cells were washed three times with PBS and permeabilized with 0.1% Triton X-100 PBS for 4 min at room temperature, washed three times with PBS and incubated with 4G2 antibodies for 30 min at 37 °C. Cells were washed three times with PBS and incubated with anti-mouse HRP-conjugated antibodies for 1 h at 37 °C. Foci were then revealed using diaminobenzidine (Sigma) (previously described in Despres et al., 1993).

YFV was titrated by plaque assay. One day before titration, Vero cells were seeded in 24 well plates. One day after seeding, 10 fold serial dilutions of infected supernatants in 2% FCS DMEM from 10^{-1} to 10^{-6} were prepared. Cells were washed three times with DMEM without FCS and 200 µl of 2% FCS DMEM were added to each well. 200 µl of dilutions 10^{-3} to 10^{-6} were then added and cells were incubated for 2 h at 37 °C. In the meantime, a 1:1 solution of CMC and 4% FCS DMEM was made and 400 µl were added to each well. Cells were then incubated at 37 °C for 5 days. Cells were washed three times in PBS and colored with 3% formaldehyde crystal violet for 20 min at room temperature. Cells were washed with water and plaques were counted.

Acknowledgments

We thank Jost Enninga (Institut Pasteur, Paris, France), Ching-Hwa Sung (Weill Cornell Medical College, New-York City, USA), Matthieu Blanchet (Institut Pasteur, Paris, France), Dorian Counor (Institut Pasteur, Shanghai, China) and Vincent Deubel (Institut Pasteur, Shanghai, China) for help and helpful discussions during the course of this work.

We also thank Emmanuelle Perret and Christophe Machu (PFID-Imagopole, Institut Pasteur, Paris, France) for their help with confocal microscopy.

We are also thankful to Stephen M. King (University of Connecticut Health Center, Farmington, USA) and M. K. Gentry and R. Putnak (Walter Reed Army Institute of Research, Washington DC, USA) for providing us R5205 and 4G2/14E9 antibodies respectively.

References

Alonso, C., Miskin, J., Hernaez, B., Fernandez-Zapatero, P., Soto, L., Canto, C., Rodriguez-Crespo, I., Dixon, L., Escribano, J.M., 2001. African swine fever virus protein p54 interacts with the microtubular motor complex through direct binding to light-chain dynein. J. Virol. 75, 9819–9827.

Ambrose, R.L., Mackenzie, J.M., 2011. West Nile virus differentially modulates the unfolded protein response to facilitate replication and immune evasion. J. Virol. 85, 2723–2732.

Brabant, M., Baux, L., Casimir, R., Briand, J.P., Chaloin, O., Porceddu, M., Buron, N., Chauvier, D., Lassalle, M., Lecoeur, H., Langonne, A., Dupont, S., Deas, O., Brenner, C., Rebouillat, D., Muller, S., Borgne-Sanchez, A., Jacotot, E., 2009. A flavivirus protein M-derived peptide directly permeabilizes mitochondrial membranes, triggers cell death and reduces human tumor growth in nude mice. Apoptosis 14, 1190–1203.

Caignard, G., Guerbois, M., Labernardiere, J.L., Jacob, Y., Jones, L.M., Wild, F., Tangy, F., Vidalain, P.O., 2007. Measles virus V protein blocks Jak1-mediated phosphorylation of STAT1 to escape IFN-alpha/beta signaling. Virology 368, 351–362.

Campbell, K.S., Cooper, S., Dessing, M., Yates, S., Buder, A., 1998. Interaction of p59fyn kinase with the dynein light chain, Tctex-1, and colocalization during cytokinesis. J. Immunol. 161, 1728–1737.

Catteau, A., Kalinina, O., Wagner, M.C., Deubel, V., Courageot, M.P., Despres, P., 2003a. Dengue virus M protein contains a proapoptotic sequence referred to as ApoptoM. J. Gen. Virol. 84, 2781–2793.

Catteau, A., Roue, G., Yuste, V.J., Susin, S.A., Despres, P., Kalinina, O., Wagner, M.C., Deubel, V., Courageot, M.P., 2003b. Expression of dengue ApoptoM sequence results in disruption of mitochondrial potential and caspase activation. Biochimie 85, 789–793.

Chambers, T.J., McCourt, D.W., Rice, C.M., Diamond, M.S., Westaway, E.G., Goodman, M.R., Wengler, G., Allison, S.L., Stadler, K., Mandl, C.W., Kunz, C., Heinz, F.X., Schalich, J., Elshuber, S., 1990. Production of yellow fever virus proteins in infected cells: identification of discrete polyprotein species and analysis of cleavage kinetics using region-specific polyclonal antisera. Virology 177, 159–174.

Chu, J.J., Yang, P.L., 2007. c-Src protein kinase inhibitors block assembly and maturation of dengue virus. Proc. Natl Acad. Sci. U. S. A. 104, 3520–3525.

Despres, P., Frenkiel, M.P., Deubel, V., 1993. Differences between cell membrane fusion activities of two dengue type-1 isolates reflect modifications of viral structure. Virology 196, 209–219.

Douglas, M.W., Diefenbach, R.J., Homa, F.L., Miranda-Saksena, M., Rixon, F.J., Vittone, V., Byth, K., Cunningham, A.L., Mueller, S., Cao, X., Welker, R., Wimmer, E., 2004. Herpes simplex virus type 1 capsid protein VP26 interacts with dynein light chains RP3 and Tctex1 and plays a role in retrograde cellular transport. J. Biol. Chem. 279, 28522–28530.

Elshuber, S., Allison, S.L., Heinz, F.X., Mandl, C.W., 2003. Cleavage of protein prM is necessary for infection of BHK-21 cells by tick-borne encephalitis virus. J. Gen. Virol. 84, 183–191.

Hirsch, A.J., Medigeshi, G.R., Meyers, H.L., DeFilippis, V., Fruh, K., Briese, T., Lipkin, W.I., Nelson, J.A., 2005. The Src family kinase c-Yes is required for maturation of West Nile virus particles. J. Virol. 79, 11943–11951.

Hsieh, S.C., Zou, G., Tsai, W.Y., Qing, M., Chang, G.J., Shi, P.Y., Wang, W.K., 2011. The C-terminal helical domain of dengue virus precursor membrane protein is involved in virus assembly and entry. Virology 410, 170–180.

Jacob, Y., Badrane, H., Ceccaldi, P.E., Tordo, N., 2000. Cytoplasmic dynein LC8 interacts with lyssavirus phosphoprotein. J. Virol. 74, 10217–10222.

Konishi, E., Mason, P.W., 1993. Proper maturation of the Japanese encephalitis virus envelope glycoprotein requires cosynthesis with the premembrane protein. J. Virol. 67, 1672–1675.

Lambert, C., Prange, R., 2003. Chaperone action in the posttranslational topological reorientation of the hepatitis B virus large envelope protein: implications for translocational regulation. Proc. Natl Acad. Sci. U. S. A. 100, 5199–5204.

Lindenbach, B.D., Thiel, H.J., Rice, C.M., 2007. Flaviviridae: the viruses and their replication, In: Knipe, D.M., Howley, P.M. (Eds.), Fields Virology, Fifth ed. Lippincott-Raven, Philadelphia, PA, pp. 1102–1152.

Lorenz, I.C., Allison, S.L., Heinz, F.X., Helenius, A., 2002. Folding and dimerization of tick-borne encephalitis virus envelope proteins prM and E in the endoplasmic reticulum. J. Virol. 76, 5480–5491.

Mackenzie, J.M., Westaway, E.G., 2001. Assembly and maturation of the flavivirus Kunjin virus appear to occur in the rough endoplasmic reticulum and along the secretory pathway, respectively. J. Virol. 75, 10787–10799.

Medigeshi, G.R., Lancaster, A.M., Hirsch, A.J., Briese, T., Lipkin, W.I., Defilippis, V., Fruh, K., Mason, P.W., Nikolich-Zugich, J., Nelson, J.A., 2007. West Nile virus infection activates the unfolded protein response, leading to CHOP induction and apoptosis. J. Virol. 81, 10849–10860.

Mendoza, J.A., Jacob, Y., Cassonnet, P., Favre, M., 2006. Human papillomavirus type 5 E6 oncoprotein represses the transforming growth factor beta signaling pathway by binding to SMAD3. J. Virol. 80, 12420–12424.

Mueller, S., Cao, X., Welker, R., Wimmer, E., 2002. Interaction of the poliovirus receptor CD155 with the dynein light chain Tctex-1 and its implication for poliovirus pathogenesis. J. Biol. Chem. 277, 7897–7904.

Ohka, S., Matsuda, N., Tohyama, K., Oda, T., Morikawa, M., Kuge, S., Nomoto, A., 2004. Receptor (CD155)-dependent endocytosis of poliovirus and retrograde axonal transport of the endosome. J. Virol. 78, 7186–7198.

Parquet, M.C., Kumatori, A., Hasebe, F., Morita, K., Igarashi, A., 2001. West Nile virus-induced bax-dependent apoptosis. FEBS Lett. 500, 17–24.

Parquet, M.C., Kumatori, A., Hasebe, F., Mathenge, E.G., Morita, K., 2002. St. Louis encephalitis virus induced pathology in cultured cells. Arch. Virol. 147, 1105–1119.

Pellet, J., Tafforeau, L., Lucas-Hourani, M., Navratil, V., Meyniel, L., Achaz, G., Guironnet-Paquet, A., Aublin-Gex, A., Caignard, G., Cassonnet, P., Chaboud, A., Chantier, T., Deloire, A., Demeret, C., Le Breton, M., Neveu, G., Jacotot, L., Vaglio, P., Delmotte, S., Gautier, C., Combet, C., Deleage, G., Favre, M., Tangy, F., Jacob, Y., Andre, P., Lotteau, V., Rabourdin-Combe, C., Vidalain, P.O., 2010. ViralORFeome: an integrated database to generate a versatile collection of viral ORFs. Nucleic Acids Res. 38, D371–D378.

Petit, C., Giron, M.L., Tobaly-Tapiero, J., Bittoun, P., Real, E., Jacob, Y., Tordo, N., De The, H., Saib, A., 2003. Targeting of incoming retroviral Gag to the centrosome involves a direct interaction with the dynein light chain 8. J. Cell Sci. 116, 3433–3442.

Prange, R., Streeck, R.E., 1995. Novel transmembrane topology of the hepatitis B virus envelope proteins. EMBO J. 14, 247–256.

Puthalakath, H., Huang, D.C., O'Reilly, L.A., King, S.M., Strasser, A., 1999. The proapoptotic activity of the Bcl-2 family member Bim is regulated by interaction with the dynein motor complex. Mol. Cell 3, 287–296.

Raux, H., Flamand, A., Blondel, D., 2000. Interaction of the rabies virus P protein with the LC8 dynein light chain. J. Virol. 74, 10212–10216.

Stadler, K., Allison, S.L., Schalich, J., Heinz, F.X., 1997. Proteolytic activation of tick-borne encephalitis virus by furin. J. Virol. 71, 8475–8481.

Su, Y., Qiao, W., Guo, T., Tan, J., Li, Z., Chen, Y., Li, X., Li, Y., Zhou, J., Chen, Q., 2010. Microtubule-dependent retrograde transport of bovine immunodeficiency virus. Cell. Microbiol. 12, 1098–1107.

Tai, A.W., Chuang, J.Z., Sung, C.H., 1998. Localization of Tctex-1, a cytoplasmic dynein light chain, to the Golgi apparatus and evidence for dynein complex heterogeneity. J. Biol. Chem. 273, 19639–19649.

Vlach, J., Lipov, J., Rumlova, M., Veverka, V., Lang, J., Srb, P., Knejzlik, Z., Pichova, I., Hunter, E., Hrabal, R., Ruml, T., 2008. D-retrovirus morphogenetic switch driven by the targeting signal accessibility to Tctex-1 of dynein. Proc. Natl Acad. Sci. U. S. A. 105, 10565–10570.

Wang, P.G., Kudelko, M., Lo, J., Siu, L.Y., Kwok, K.T., Sachse, M., Nicholls, J.M., Bruzzone, R., Altmeyer, R.M., Nal, B., 2009. Efficient assembly and secretion of recombinant subviral particles of the four dengue serotypes using native prM and E proteins. PLoS One 4, e8325.

Wang, X., Olberding, K.E., White, C., Li, C., 2011. Bcl-2 proteins regulate ER membrane permeability to luminal proteins during ER stress-induced apoptosis. Cell Death Differ. 18, 38–47.

Wengler, G., 1989. Cell-associated West Nile flavivirus is covered with E + pre-M protein heterodimers which are destroyed and reorganized by proteolytic cleavage during virus release. J. Virol. 63, 2521–2526.

Westaway, E.G., Goodman, M.R., 1987. Variation in distribution of the three flavivirus-specified glycoproteins detected by immunofluorescence in infected Vero cells. Arch. Virol. 94, 215–228.

Yu, C.Y., Hsu, Y.W., Liao, C.L., Lin, Y.L., 2006. Flavivirus infection activates the XBP1 pathway of the unfolded protein response to cope with endoplasmic reticulum stress. J. Virol. 80, 11868–11880.

Yu, I.M., Holdaway, H.A., Chipman, P.R., Kuhn, R.J., Rossmann, M.G., Chen, J., 2009. Association of the pr peptides with dengue virus at acidic pH blocks membrane fusion. J. Virol. 83, 12101–12107.